Vol. 486: 247–256, 2013
doi: 10.3354/meps10328

MARINE ECOLOGY PROGRESS SERIES
Mar Ecol Prog Ser

Published July 12

Effect of laser ablation depth in otolith life history scans

Reneé R. Hoover[1,2,*], Cynthia M. Jones[1]

[1]Center for Quantitative Fisheries Ecology, Norfolk, Virginia 23508, USA
[2]*Present address:* Virginia Marine Resources Commission, Newport News, Virginia 23607, USA

ABSTRACT: Life history scans of fish otoliths are bringing new insight into the structure, connectivity, and movement of fish populations. Data obtained from such scans, however, possess inherent limitations that have not yet been fully addressed or understood. For example, several investigators have noted delays in otolith elemental uptake that do not appear to reflect habitat exposure. We hypothesized that the 3-dimensional structure of otoliths may produce sampling artifacts in the results obtained from laser ablation scans. To test this hypothesis, we sampled sagittal otoliths from juvenile Atlantic croaker *Micropogonias undulatus* with laser ablation inductively coupled plasma mass spectrometry to obtain elemental molar ratios of a common environmental marker (barium). We ablated 2 trenches of different depths on each otolith and performed spectral analyses on the data to investigate the effects of ablation depth, including differences in the periodicities and temporal variability between trenches. The mean barium concentration between the 2 trenches was significantly different ($t = 114.25$, $p < 0.0001$). From shallow to deep trenches, variance decreased; the standard error about the means was reduced from 0.609 to 0.086. Peaks in spectral density, which estimate the ingress timing for this species, were shifted in absolute value an average of 32 d. Our results highlight the necessity of considering depth of laser ablation when conducting life history scans.

KEY WORDS: Life history scan · LA-ICPMS · Lag effect · Otolith chemistry

Resale or republication not permitted without written consent of the publisher

INTRODUCTION

Otolith life history scans have proven to be powerful tools for providing information about fish population movements and structure (Campana 1999, Thorrold et al. 2001, Ashford et al. 2012). As with any developing technique, however, caution must be exercised in advancing such applications. The intrinsic limitations of using otoliths as natural tags have not yet been fully addressed or understood. The present study focuses on issues in life history scan methods that arise from the 3-dimensional nature of otolith morphology.

Fisheries scientists often rely on conceptual models to describe methods of analyzing fish life histories, such as the ability to estimate age and growth using otoliths. The most common conceptual model to describe the morphology of otoliths is that of tree rings. Considering the long history of silviculture and ageing of trees with annuli, this conceptual model for ageing otoliths and extracting information from their increments is practical. With the tree ring concept, each cross-section has concentric layers; a cut made at the top of the structure theoretically contains the same number of layers as a cut made through the center (Fig. 1a). Otoliths, however, have layers which curve around and underneath, much more like an onion. A slice taken from the top of the onion will not necessarily have the same number of rings as a slice taken through the center. Fig. 1b illustrates an otolith half in the typical preparation for use in a life history scan. By changing the conceptual diagram from a

*Email: renee.hoover@mrc.virginia.gov

© Inter-Research 2013 · www.int-res.com

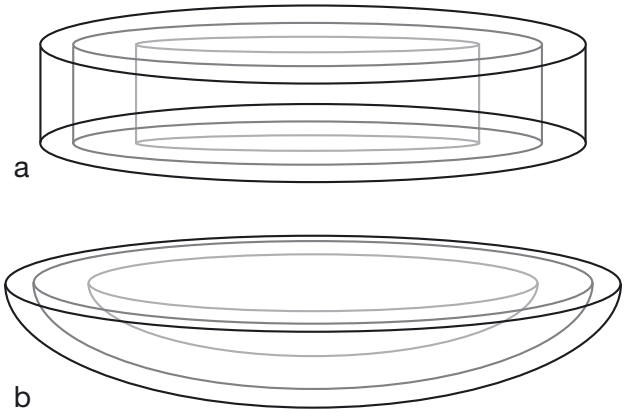

Fig. 1. (a) Section of a tree-like structure, where cuts at the top, middle, and bottom of the structure all contain the same number of rings; (b) half of an onion-like structure (otolith), where layers curve around and underneath. A cut at the top or bottom will not contain the same number of rings as a cut in the middle. (Illustration by Bob Jones)

cylinder (i.e. a tree) to a sphere, we emphasize a third dimension of the otolith: depth.

For certain areas of otolith research, morphology may not play an important role; when conducting life history scans, however, it may be significant. The scan itself can occur at considerable depth within the otolith depending on the method used. If the depth of ablation is not considered and accounted for in these analyses, the inherent assumption is that ablation depth will not influence chemical signatures. While this assumption is valid for surface scans using wave-dispersive microprobes, with depths of 1 to 3 µm (Zlokovitz et al. 2003), it may be violated if the scan occurs at deeper depth. For example, certain laser scans may ablate as deep as 300 µm (Jones & Chen 2003). Thus, depth may be an issue if a scan is being conducted on an entire otolith half, as is often the case (Ben-Tzvi et al. 2008, Hale & Swearer 2008, Standish et al. 2008).

One widely used method for conducting otolith life history scans is laser ablation inductively coupled plasma mass spectrometry (LA-ICPMS), which involves ablating a trench into the otolith across its increments. Using this method, one obtains a scan from the beginning of the fish's life, at the core of the otolith, through to the date of capture, at the edge. The dashed horizontal arrow in Fig. 2 demonstrates a cross-section of this trench. When a deeper trench is made, however, one may be ablating material not only across layers but also through them. Doing so incorporates more growth increments than desired, as is seen by the solid arrow in Fig. 2.

Despite increasing popularity of using laser ablation to obtain life history scans, previous studies have largely ignored the depth of ablation. In a sample of 12 recent LA-ICPMS otolith chemistry papers, only 1 (Kemp et al. 2011) reported laser ablation depth in its methods, and very few papers microscopically validate ablation depths. In some studies, such as Ruttenberg et al. (2005), ablation depth was indirectly

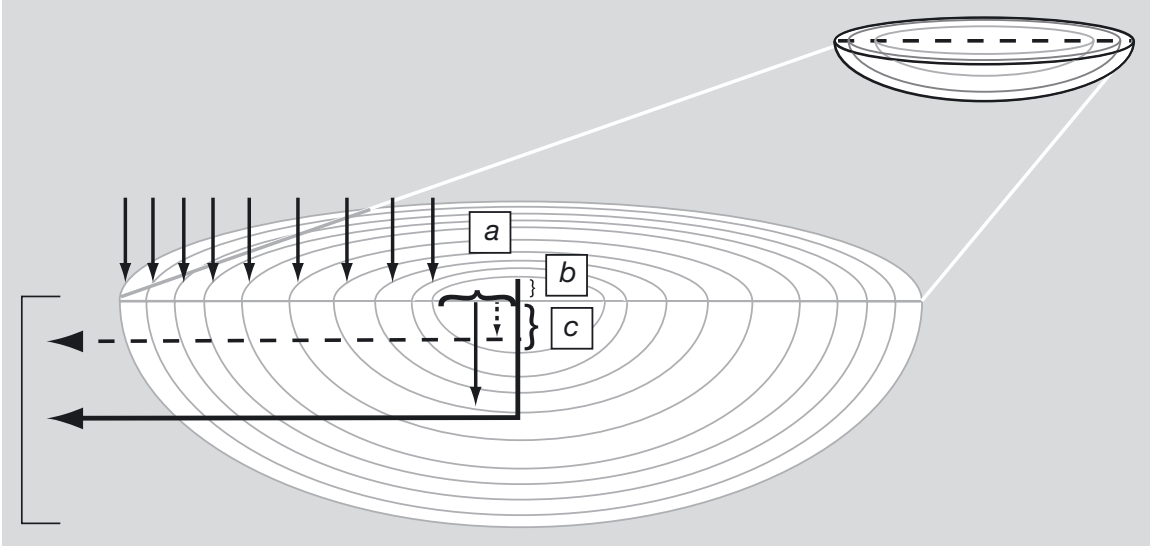

Fig. 2. Stylized cross-section of an otolith half. The small inset is a depiction of the otolith half from which the larger cross-section is taken. The arrows coming down across the top of the half represent the laser: the dashed arrow represents a shallow laser ablation trench, and the solid arrow represents a deeper trench. Labels in each spatial plane relate to the equation of the general ellipse. (Illustration by Bob Jones)

accounted for by repeatedly pulsing the laser in a series of small, discrete pits at the otolith core. The goal of these studies was not to complete a life history scan, however; the laser was instead used to isolate and characterize the juvenile portion of the otolith for natal habitat identification.

The lack of attention to laser ablation depth is a potential cause for concern in otolith chemistry investigations. Specifically, fisheries ecology studies have reported lag effects in strontium uptake as well as saturation levels in otolith uptake (Elsdon & Gillanders 2005a, Macdonald & Crook 2010, Miller 2011). While these studies help us to comprehend the link between ambient strontium levels and otolith elemental concentrations, some of these results may be sampling artifacts of how the life history scans were performed, and the 'lag effect' in uptake may not in fact be real. The concept of delayed uptake, by as much as 40 d, runs counter to studies in the physiological literature that demonstrate uptake of radiolabeled elements onto the otolith within several hours (Mugiya & Tanaka 1995, Skov et al. 2001). Moreover, if a scan were taken at an ablation depth that crossed many increments of growth in the vertical plane, the signal could be an integration of several life history stages, with no quantitative measure of the level of integration or the bias that such integration would introduce. By examining the conceptual models used in this area of otolith research, i.e. 2-dimensional tree rings versus 3-dimensional onions, a new level of understanding is reached in how the mechanics of laser ablation sampling might affect otolith chemistry results.

The effect of ablating through layers on trace element signatures has not yet been investigated experimentally. The purpose of the present study was to examine how the depth of ablation affects elemental chemistry results. We hypothesized that the distance between the polished surface and the bottom of the ablation trench would change the number of increments sampled, causing more recent layers to be sampled with deeper ablation depths. We tested the null hypothesis that depth of ablation will not influence chemical signatures through a comparison between shallow and deep otolith chemistry signatures using LA-ICPMS.

Because of the longitudinal nature of these data, we analyzed the results using the time series techniques described by Hoover et al. (2012). Doing so makes use of the full environmental chronology contained in each life history scan while maintaining the temporal resolution and statistical accuracy of our data analysis.

MATERIALS AND METHODS

Sample preparation and analysis

We performed the elemental analysis using sagittal otoliths of juvenile Atlantic croaker *Micropogonias undulatus*. Atlantic croaker are found in demersal, brackish, and marine habitats, from 43° N to 37° S. Based on the work of Hettler (1998), Warlen & Burke (1990), and Hoskin (2002), we expect croaker will show a strong shift in their otolith chemistry at the time of ingress into the estuarine environment, at approximately 90 d. The fish we analyzed were a subsample of individuals from the Pamlico River in North Carolina, USA, captured during April and May of 1997 (n = 14).

One sagittal otolith from each fish was chosen at random (left or right) for elemental analysis, and the second otolith was used for ageing. We prepared all otoliths for trace element analysis in a Class 100 clean room, cleaning the samples of any attached tissue and rinsing in ultrapure hydrogen peroxide and ultrapure Milli-Q water. Trace element analysis followed the methods described in Hoover et al. (2012), with 3 calibration standards synthesized from stock single element and multi-element standards at concentrations typically observed in otoliths at the beginning and end of each sequence as well as a certified otolith reference material (Yoshinaga et al. 2000) and instrumental blanks of 5% HNO_3 interspersed throughout each block of otoliths. Based on the results of Hoover et al. (2012), we concluded that barium provided the best marker to assess the effects of laser depth on resulting element concentrations. The 2 elements analyzed were barium (^{138}Ba) and calcium (^{48}Ca) scanned in low-resolution mode (Taylor 2001, Chen & Jones 2006). We converted the raw data to element-to-calcium molar ratios.

The following depth model was developed (Jones & Chen 2003) for the MAT Element 2 ICPMS (Finnigan) at Old Dominion University's Laboratory for Isotope and Trace Element Research:

$$\text{crater depth} = 19 + 1.4 \times \text{power} - 0.4 \times \text{travel speed} \quad (1)$$

where crater depth is in micrometers, power is in percent, and travel speed is in micrometers per second. We used this equation to determine the power levels necessary to obtain our desired trench depths. We ablated a line from the core of the otolith towards the edge to obtain a series of the trace element signatures representing each individual's life history. Two trenches were made directly adjacent and parallel to

one another along the transect. To obtain 2 different depths, holding speed (5 µm s^{-1}) and spot size (20 µm) constant, we used 45 and 100% power to obtain scans at 80 and 160 µm, respectively. These depths were verified microscopically.

We cut transverse thin sections from the otoliths for age and growth analyses. Sections were mounted and polished to reveal the core for ageing of daily growth increments. We measured daily increment widths using ImagePro Version 5.0.1 software. The daily ages and increments were measured on the same sample and used in subsequent growth rate estimation to transform the life history scan data into a temporal scale in terms of the days in a given fish's life (Hoover et al. 2012).

Data analysis

Because the data obtained from these analyses are time series, applying traditional parametric statistics to compare the 2 ablation depths would not be appropriate. We therefore conducted a spectral analysis following the methods in Hoover et al. (2012) to quantitatively analyze the effects of trench depth on elemental concentrations. We used a low-pass filter to remove the components of the series not adding information to our analysis, with the cutoff at $f\Delta t$ = 0.3. Trend components were modeled by fitting either a linear

$$X_j = A_1 + B_1 t_j \quad (2)$$

or quadratic function

$$X_j = A_2 + B_2 t_j + C_2 t_j^2 \quad (3)$$

We tested for the significance of the trend component by calculating the variance before and after the fit and using an *F*-test to decide if the variances were significantly different.

Subsequently, we standardized the data by dividing each series by its standard deviation, which allowed us to compare series with widely varying levels of stochasticity. We calculated spectral density estimates using the Maximum Entropy Method (MEM) as described by Press et al. (1994). Details of the application of the above methods are described in Hoover et al. (2012).

To compare the overall means between the 2 trenches, we performed both a paired *t*-test and a mixed-effects ANOVA. The mixed-effects ANOVA is appropriate in this case because we are dealing with both fixed and random effects. The fixed effect is the trench depth, since our sampling fraction for that variable is 1 (we are sampling the entire population of possible depths, because we were only interested in shallow versus deep trenches). The random effect is the individual, as this sampling fraction is <1; we are analyzing some subsample of the entire population of Atlantic croaker being considered.

We also examined the maximum peak in spectral density for both depths. The highest peak in spectral density represents the most significant frequency component of the signal and consequently measures the point in time with the highest probability of transition from one habitat (saline) to the next (estuarine). Thus, we use the peak in spectral density as a proxy for the timing of ingress to the estuary. We compared and tested for significant differences in the timing of ingress between the 2 depths using a paired *t*-test. Paired *t*-tests and the mixed-effects ANOVA were conducted in SAS version 9.2.

Finally, we can model the number of layers that will be incorporated for a given depth by assuming a known shape to approximate the morphology of the otolith. The most generalized conceptual model of otolith growth would be a sphere. The oversimplified example of a sphere dramatically underestimates the number of increments ablated and is grossly conservative; however, we use it to illustrate the conceptual point directly. We measure the width of the increments when ageing the fish. By assuming spherical growth, we can calculate the quantity in the vertical plane that corresponds to a given increment width in the horizontal plane; in a sphere, these measurements would be equal in all directions. Again, we make this example bearing well in mind that in most real otoliths, more material accumulates in the horizontal plane (from anterior to posterior, and dorso-ventrally) than in the vertical plane.

For a conservative example, we conducted our analysis on a sciaenid with fast-growing otoliths; our mean otolith increment width for the first day outside of the core is 8 µm. Assuming the otolith's morphology to be a sphere with constant increment width, a trench depth of 160 µm would exceed our first increment of growth by 20 times. Understanding that most otoliths are not spherical but rather more elliptical in shape, as in Fig. 2, and that increment widths are not constant, it can easily be seen that our vertical axis is even further compressed with respect to the horizontal plane, which incorporates more recent material.

The surface area of a general (tri-axial) ellipsoid is

$$S = 2\pi c^2 + \frac{2\pi ab}{\sin\varphi}[E(\varphi,k)\sin^2\varphi + F(\varphi,k)\cos^2\varphi] \quad (4)$$

where

$$\varphi = \arccos\left(\frac{c}{a}\right),\ k^2 = \frac{a^2(b^2 - c^2)}{b^2(a^2 - c^2)},\ a \geq b \geq c \qquad (5)$$

given that a, b and c are the semi-principal axes of the ellipsoid and $F(\varphi,k)$ and $E(\varphi,k)$ are incomplete elliptic integrals of the first and second kind, respectively.

Therefore, given an increment width, c, along the same transect used for ablation, we can solve for the depth, a, that the layer runs around and underneath. If the ablation depth exceeds that amount, the scan results will be incorporating at least that much material at a given point in time along the laser transect.

Each increment is measured in the horizontal plane, and therefore those measurements can be used to describe the b and c measurements, accounting for the unequal increment widths between years. The amount of material (or number of increments) ablated in the vertical plane, then, is equal to c in Eqs. (4) & (5). Again, we provide this simple example to illustrate how easily laser ablation can integrate over several growth increments when conducting a life history scan. Looking back to the conceptual diagram of Fig. 2, the increased potential of ablating through layers in the vertical plane, where the c measurement occurs, is clear.

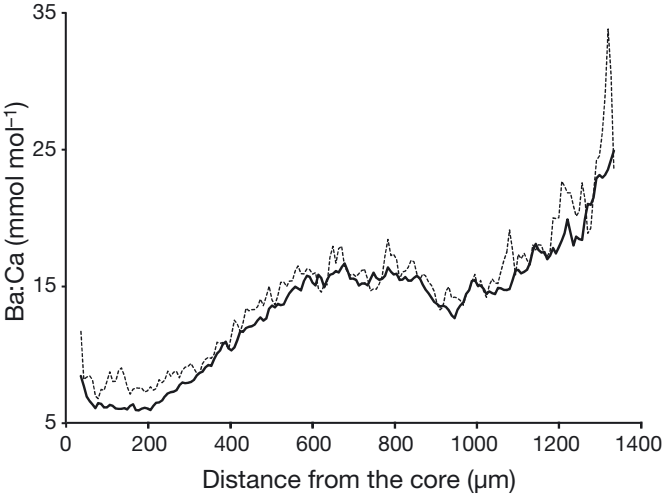

Fig. 3. Barium-to-calcium ratios plotted against distance from the core of the otolith to the edge. The dashed line is the shallow (80 µm) trench, and the solid line is the deep (160 µm) trench

RESULTS

Elemental concentrations

We analyzed 2 trench depths, one shallow (80 µm) and one deep (160 µm), for 2 elements (^{138}Ba and ^{48}Ca) on 14 fish. Fish ranged in size from 41 to 70 mm standard length, with ages ranging from 78 to 145 d. Otoliths ranged in diameter from 1064 to 1891 µm.

A representative plot of the raw barium-to-calcium data for both shallow (dashed line) and deep (solid line) scans is shown in Fig. 3. The expected trend from low to high barium concentrations, as the fish moves from saline to estuarine waters, appears clearly. Shallow barium values ranged from 7.29 (±6.54) mmol mol^{-1} at the core to 10.23 (±7.44) mmol mol^{-1} at the edge at the time of capture. The deep trench barium values ranged from 7.47 (±6.55) mmol mol^{-1} at the core to 11.20 (±6.99) mmol mol^{-1} at the edge. The paired t-test showed overall significant differences between mean shallow and deep barium values (t = 114.25, p < 0.0001) within each fish.

Deep scans consistently exhibit less variable results as compared to shallow scans on the same individual. We noted that the highest peaks and lowest troughs in raw element-to-calcium molar ratios always appeared in the shallow trench data, as is seen in Fig. 3. The overall variance of the data diminished dramatically from the shallow (SD = 34.919 mmol mol^{-1}) to deep (SD = 4.944 mmol mol^{-1}) barium data, and the standard error about the means was reduced from 0.609 to 0.086.

Spectral analysis

We conducted spectral analysis on the shallow and deep data using Ba:Ca for each sample. The highest peak in spectral density represents the most significant periodic component of a life history scan signal, in this case representing the timing of transition between the marine and estuarine environments (i.e. ingress timing). Results of the spectrally derived ingress times and differences between shallow and deep estimates are summarized in Table 1, along with the overall means and their associated standard deviations.

The spectral density plots for barium are shown in Fig. 4 with both shallow (dashed) and deep (solid line) data for each individual. The estimated ingress timing was significantly different between shallow and deep data using the paired t-test (t = 6.14, p < 0.0001). The mixed-effects ANOVA also showed significant differences for the fixed effect of depth for barium (F = 18.46, p = 0.0002). Fig. 5 displays the resultant distribution of ingress times estimated by the shallow and deep trenches for barium. Note the

Table 1. Spectrally derived estimates of ingress timing (in days)

Sample	Age	Ba		Difference
		Shallow	Deep	
1	78	26	16	10
2	99	61	30	30
3	120	83	36	47
4	137	91	91	0
5	110	74	31	43
6	136	91	74	17
7	120	95	48	48
8	110	74	69	5
9	136	91	56	35
10	139	91	45	45
11	145	95	83	12
12	110	74	28	46
13	127	91	43	47
14	134	91	29	61
Mean	121.5	80.6	48.6	32.0
SD	18.6	18.7	22.9	19.5

difference in shapes between the shallow and deep distributions, with a negatively skewed shape for the shallow relative to the deep ingress times.

Additionally, we note that there was a lag in the overall timing of ingress as estimated using the shallow ablation depth data when compared to the ingress timing from the deep data. The mean lag in estimated ingress timing comparing shallow with respect to deep data was 32 ± 19.5 d.

DISCUSSION

We demonstrate that when using laser ablation, the transect depth significantly affects the chemical signatures obtained from life history scans of otoliths. Using LA-ICPMS to conduct life history scans, we directly compared chemical signatures from shallow and deep ablation depths. We saw a significant dif-

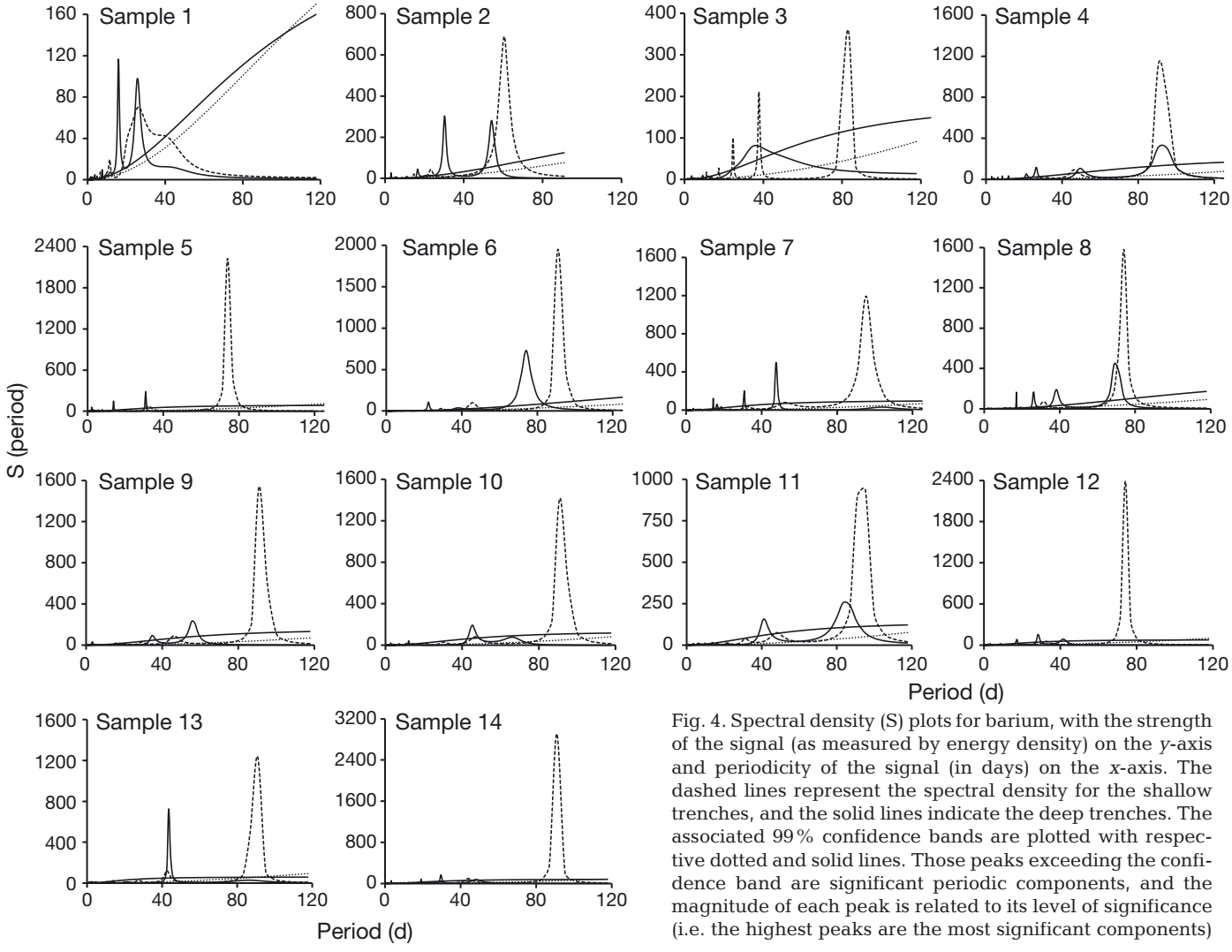

Fig. 4. Spectral density (S) plots for barium, with the strength of the signal (as measured by energy density) on the *y*-axis and periodicity of the signal (in days) on the *x*-axis. The dashed lines represent the spectral density for the shallow trenches, and the solid lines indicate the deep trenches. The associated 99% confidence bands are plotted with respective dotted and solid lines. Those peaks exceeding the confidence band are significant periodic components, and the magnitude of each peak is related to its level of significance (i.e. the highest peaks are the most significant components)

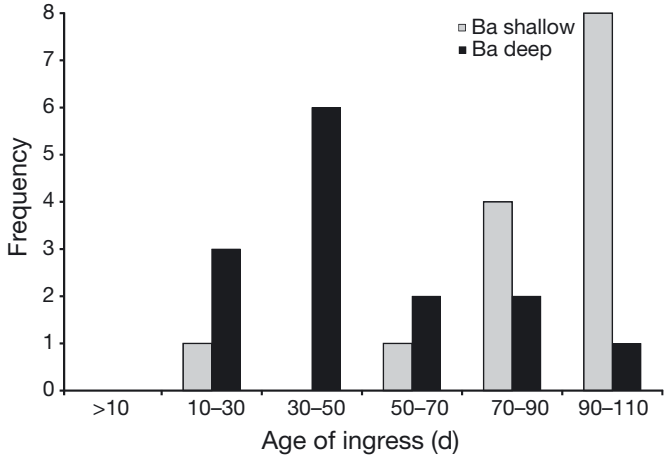

Fig. 5. Distribution of estimated ingress timing based on barium values using both shallow and deep data

ference in the raw element-to-calcium molar ratios between the 2 trench depths. These results illustrate the critical role of depth in understanding the spatial heterogeneity of elemental signatures throughout the otolith when analyzed using laser ablation.

Comparing the spatial differences between the 2 trenches, the visible smoothness of deeper trench data is consistent among all samples (e.g. Fig. 3). This smoothing effect is likely because a deeper trench samples through several incremental layers, so that each data point in the signal integrates over more growth bands rather than each individual layer. In effect, the trace elemental signature is being averaged by the surrounding layers. This is reflected in the decrease in variance seen in the deeper layers of our samples, in the same way that variance decreases between any raw data and a moving average estimate. Additionally, we consider the possibility that ablating a deeper trench introduces a larger amount of material into the instrument, potentially creating a more stable signal.

By using the spectral approach in Hoover et al. (2012), we further investigated the effects of ablation depth on these data by estimating the timing of ingress for each individual. We hypothesized that the overall effect across a known salinity gradient would be a shift in the estimated ingress timing, as calculated through the spectral analysis of the barium signals. Barium exhibited significant differences in the estimated timing of ingress (Fig. 4), with a skew towards earlier ingress time using the deeper trench data (Fig. 5). Peaks detected in the shallow trench matched empirical collections of Hettler (1998) and Warlen & Burke (1990) of 90 d ingress. This early skew in deep trench data demonstrates that barium-richer layers were prematurely incorporated into putatively 'early' sampling, thus anticipating fish movement up-estuary.

In addition to the vertical integration resulting from the depth of laser ablation, the second means of integration that physically results from this sampling method is in the horizontal (x, y) plane due to the spot size of the laser. Though not directly quantified, we note the importance of considering increment width relative to the spot size of the laser, particularly with larval and juvenile fish and those fishes with small or thin otolith morphologies. Given the relatively large size of juvenile Atlantic croaker otoliths and wide increment widths, the spot size of 25 µm likely integrated on the order of a single day, as our mean increment width for all samples was 17 (±6) µm. Considering that this species is a fast-growing sciaenid, we stress that any generalizations concerning integration across or through increments are conservative in nature. In an otolith with narrower increment widths, however, the integration over several days in the horizontal plane could present an integration problem similar to the one we describe in the vertical (z) plane in Fig. 2 and through the conceptual volume equations (Eqs. 1 to 5) for ellipsoids provided in our 'Materials and methods' section.

These 2 cases of integration demonstrate important potential impacts of the physical aspects of laser ablation on life history scan results, particularly in studies investigating the timing of fish movement through environmental gradients. Those studies which attempt to reconstruct environmental histories using LA-ICPMS data require deliberate consideration of ablation dimensions in their analysis. Papers in the otolith chemistry literature suggest that a lag effect in the incorporation of strontium (Elsdon & Gillanders 2005a, Macdonald & Crook 2010) and barium (Macdonald & Crook 2010, Miller 2011) may be occurring. These studies report up to a 40 d lag in the incorporation of elements into the otolith. These results strongly contrast the historical physiology literature, which reports almost immediate incorporation of minor and trace elements into the otolith microchemistry (Farrell & Campana 1996). As follows from the work of Mugiya et al. (1991), establishing the incorporation of trace metals into otoliths, as well as the biophysiological studies conducted by Payan et al. (2004) and the precipitation kinetics investigation of Romanek & Gauldie (1996), the incorporation of trace elements into the otolith should occur on the order of 24 to 48 h. Even more specifically, Borelli et al. (2003) conclude that $CaCO_3$ precipitation should occur when saturation is reached, at the end of the night.

These physiological studies offer no support for the presence of either a lag effect in uptake or an organ where strontium and barium are stored to be released later. The discrepancy between the physiological and ecological studies raises concerns for whether lag effects are in fact present in the otolith chemistry. We fully appreciate that different pathways for elemental uptake between marine and freshwater environments, i.e. through the intestinal wall versus gill membranes (Wells et al. 2003, Zimmerman 2005), have the potential to affect uptake dynamics. If a lag in uptake is present, however, there must be a physiological explanation for why that lag occurs, particularly in the face of previous work demonstrating almost immediate elemental uptake. Moreover, our data show that if ablation depth is not considered, an artificial lag may be introduced, further confounding the estimates of movement timing. Although we cannot dismiss the possibility of valid lag effects in elemental uptake, the most parsimonious explanation is that lags seen in laser ablation studies are sampling artifacts and could result from an effect as simple as ablation depth.

We hypothesized that the discrepancy seen in our data when examining not only variability of the data but also ingress timing itself would be a powerful indicator of the effect of ablation depth on otolith chemistry results. Our data show different timing of element uptake, depending on ablation depth. Specifically, our data show higher barium concentrations sooner than would be expected, as fish move from lower to higher concentrations, and barium-estimated ingress time differs by approximately 2 wk in the deeper trench data. Whether the elemental change occurs earlier or later than it should in reality will depend on whether the concentration gradient is positive or negative and on the shape of the otolith. The key is that the 2 sampling depths produced different results, leading to different conclusions regarding ingress time.

While several issues exist in obtaining accurate microchemical data from otoliths, our study has particular implications for morphological considerations. If the otolith being analyzed by a technique that samples deeply is ovoid in shape, then material will be accumulated around the otolith fairly evenly as the fish grows. In this case, using a sciaenid species, the morphology provides a somewhat muted sensitivity to ablation depths because growth layers are more uniform. In contrast, otoliths that are long and thin pose more of a problem for life history scans using LA-ICPMS because for a given depth, more growth layers are present to be ablated and this is exacerbated at the edges of these otoliths. Because of this morphology, the danger of ablating through more layers instead of only across them is much greater. Unfortunately, some of the world's most valuable fish have long, thin otolith morphologies, making them more susceptible to microchemistry measurement errors and, consequently, conclusions drawn from these analyses.

Such limitations on otolith chemistry investigations with laser-based ICPMS argue for the use of surface-sampling instruments such as the wave-dispersive microprobe (Secor et al. 1998). However, this approach is not without its limitations. While strontium can be valuable in evaluating some types of movement during the life history in embayments, other elements such as barium may be more useful in riverine and estuarine systems (Elsdon & Gillanders 2005b, Feutry et al. 2011). Not all life history scan investigations use laser ablation methods, but there is a predominance of this method in the otolith chemistry literature (Campana et al. 1994, Thorrold et al. 1997, Jessop et al. 2012). Although the microprobe provides estimates of strontium, other important elements such as barium are below detection limits for most otolith samples (Campana et al. 1997). There have been several successful studies investigating whether differences in life history are recorded in strontium signals (Waight et al. 2002, Milton & Chenery 2003), but we note that the wide use of LA-ICPMS also stems from its ability to detect a broad array of minor and trace elements in trace and ultra-trace concentrations (Marklevitz et al. 2011, Olley et al. 2011, Tanner et al. 2012). The limitations of these techniques continue to evolve and be investigated (De Vries et al. 2005, Ben-Tzvi et al. 2007, Elsdon et al. 2008). With time, a trend towards the use of more precise laser ablation units (193 and 213 nm systems) has developed because of their increased precision in settings with opaque and transparent materials, such as otoliths. For example, there has been success with both larval (Brophy et al. 2003) and juvenile fish (Walther & Thorrold 2008). The development of multi-collector ICPMS approaches to otolith chemistry has shown great potential, with highly accurate and precise results (Woodhead et al. 2005). Challenges in the analytical method are still present, however, with correlated changes in $^{87}Sr^{86}/Sr$ and the invariant ratio $^{84}Sr/^{86}Sr$ (Waight et al. 2002) and a need for wide ablation paths, on the order of several hundred micrometers (Milton & Chenery 2003). These general challenges are summarized in Vroon et al. (2008).

Fish otoliths are widely recognized as valuable natural recorders of life history information. While our ability to obtain information from these structures continues to increase, the inherent limitations of both our sampling techniques and data analyses must be acknowledged. The value of increasing our understanding of those limitations lies in our future ability to predict and compensate for inherent restrictions in our analyses. Since the data acquired from otolith microchemistry are used to identify nursery habitat, larval dispersal trajectories, and migratory routes, otolith chemistry studies have the potential to impact fisheries management directly. With this knowledge base and a precautionary approach, fisheries scientists may comprehend higher levels of the complex and intricate systems they seek to analyze and manage.

Acknowledgements. We thank C. Grosch, N. Diawara, D. Naik, J. J. Schaffler, S. K. Beharry, S. Turner, and all of the faculty and staff at the Center for Quantitative Fisheries Ecology. The fish in this study were collected by personnel at the Beaufort Laboratory, National Marine Fisheries Service, NOAA. This study was funded by the National Science Foundation (Project #OCE-0961421).

LITERATURE CITED

Ashford J, Dinniman M, Brooks C, Andrews AH and others (2012) Does large-scale ocean circulation structure life history connectivity in Antarctic tootfish (*Dissostichus mawsoni*)? Can J Fish Aquat Sci 69:1903–1919

Ben-Tzvi O, Abelson A, Gaines SD, Sheehy MS, Paradis GL, Kiflawi M (2007) The inclusion of sub-detection limit LA-ICPMS data, in the analysis of otolith microchemistry, by use of a palindrome sequence analysis (PaSA). Limnol Oceanogr Methods 5:97–105

Ben-Tzvi O, Kiflawi M, Gaines SD, Al-Zibdah M, Sheehy MS, Paradis GL, Abelson A (2008) Tracking recruitment pathways of *Chromis viridis* in the Gulf of Aqaba using otolith chemistry. Mar Ecol Prog Ser 359:229–238

Borelli G, Mayer-Gostan N, Merle P, Pontual HD, Boeuf G, Allemand D, Payan P (2003) Composition of biomineral organic matrices with special emphasis on turbot (*Psetta maxima*) otolith and endolymph. Calcif Tissue Int 72: 717–725

Brophy D, Danilowicz BS, Jeffries TE (2003) The detection of elements in larval otoliths from Atlantic herring using laser ablation ICP-MS. J Fish Biol 63:990–1007

Campana SE (1999) Chemistry and composition of fish otoliths: pathways, mechanisms and applications. Mar Ecol Prog Ser 188:263–297

Campana SE, Fowler AJ, Jones CM (1994) Otolith elemental fingerprinting for stock identification of Atlantic cod (*Gadus morhua*) using laser ablation ICPMS. Can J Fish Aquat Sci 51:1942–1950

Campana SE, Thorrold SR, Jones CM, Gunther D and others (1997) Comparison of accuracy, precision, and sensitivity in elemental assays of fish otoliths using the electron microprobe, proton-induced X-ray emission, and laser ablation inductively coupled plasma mass spectrometry. Can J Fish Aquat Sci 54:2068–2079

Chen Z, Jones CM (2006) Simultaneous determination of 33 major, minor, and trace elements in juvenile and larval fish otoliths by high resolution double focusing sector field inductively coupled plasma mass spectrometry. 2006 Winter Conf on Plasma Spectrochemistry, Tucson, AZ, January 8–14, 2006

De Vries MC, Gillanders BM, Elsdon TS (2005) Facilitation of barium uptake into fish otoliths: influence of strontium concentration and salinity. Geochim Cosmochim Acta 69: 4061–4072

Elsdon TS, Gillanders B (2005a) Strontium incorporation into calcified structures: separating the effects of ambient water concentration and exposure time. Mar Ecol Prog Ser 285:233–243

Elsdon TS, Gillanders B (2005b) Consistency of patterns between laboratory experiments and field collected fish in otolith chemistry: an example and applications for salinity reconstructions. Mar Freshw Res 56:609–617

Elsdon TS, Wells BK, Campana SE, Gillanders BM and others (2008) Otolith chemistry to describe movements and life-history parameters of fishes: hypotheses, assumptions, limitations and inferences. Oceanogr Mar Biol Annu Rev 46:297–330

Farrell J, Campana SE (1996) Regulation of calcium and strontium deposition on the otoliths of juvenile tilapia, *Oreochromis niloticus*. Comp Biochem Physiol A 115: 103–109

Feutry P, Keith P, Pécheyran C, Claverie F, Robinet T (2011) Evidence of diadromy in the French Polynesian *Kuhlia malo* (Teleostei: Percoidei) inferred from otolith microchemistry analysis. Ecol Freshw Fish 20:636–645

Hale R, Swearer SE (2008) Otolith microstructural and microchemical changes associated with settlement in the diadromous fish *Galaxias maculatus*. Mar Ecol Prog Ser 354:229–234

Hettler WF (1998) Abundance and size of dominant winter-immigrating fish larvae at two inlets into Pamlico Sound, North Carolina. Brimleyana 25:144–155

Hoover RR, Jones CM, Grosch CE (2012) Estuarine ingress timing as revealed by spectral analysis of life history scans. Can J Fish Aquat Sci 69:1266–1277

Hoskin S (2002) Recruitment variability of Atlantic croaker *Micropogonias undulatus*, with observations on environmental factors. MS thesis, Old Dominion University, Norfolk, VA

Jessop BM, Wang CH, Tzeng WN, You CF, Shiao JC, Lin SH (2012) Otolith Sr:Ca and Ba:Ca may give inconsistent indications of estuarine habitat use for American eels (*Anguilla rostrata*). Environ Biol Fish 93:193–207

Jones CM, Chen Z (2003) New techniques for sampling larval and juvenile fish otoliths for trace-element analysis with laser-ablation sector-field inductively-coupled-plasma mass spectrometry (SF-ICP-MS). In: Browman HI, Skiftesvik AB (eds) The big fish bang. Proc 26th Annu Larval Fish Conf. Institute of Marine Research, Bergen, p 431–443

Kemp J, Swearer SE, Jenkins GP, Robertson S (2011) Otolith chemistry is more accurate than otolith shape in identifying cod species (genus *Pseudophycis*) in the diet of Australian fur seals (*Arctocephalus pusillus doriferus*). Can J Fish Aquat Sci 68:1732–1743

Macdonald JI, Crook DA (2010) Variability in Sr:Ca and Ba:Ca ratios in water and fish otoliths across an estuarine salinity gradient. Mar Ecol Prog Ser 413:147–161

Marklevitz SAC, Fryer BJ, Gonder D, Yang ZP, Johnson J, Moerke A, Morbey YE (2011) Use of otolith chemistry to discriminate juvenile Chinook salmon (*Oncorhynchus tshawytscha*) from different wild populations and hatcheries in Lake Huron. J Gt Lakes Res 37:698–706

Miller J (2011) Effects of water temperature and barium concentration on otolith composition along a salinity gradient: implications for migratory reconstructions. J Exp Mar Biol Ecol 405:42–52

Milton DA, Chenery SR (2003) Movement patterns of the tropical shad hilsa (*Tenualosa ilisha*) inferred from transects of 87Sr/86Sr isotope ratios in their otoliths. Can J Fish Aquat Sci 60:1376–1385

Mugiya Y, Tanaka S (1995) Incorporation of water-borne strontium into otoliths and its turnover in the goldfish *Carassius auratus*: effects of strontium concentrations, temperature, and 17β-estradiol. Fish Sci 61:29–35

Mugiya Y, Hakomori T, Hatsutori K (1991) Trace metal incorporation into otoliths and scales in the goldfish, *Carassius auratus*. Comp Biochem Physiol C 99:327–331

Olley R, Young RG, Closs GP, Kristensen EA and others (2011) Recruitment sources of brown trout identified by otolith trace element signatures. NZ J Mar Freshw Res 45:395–411

Payan P, De Pontual H, Bœuf G, Mayer-Gostan N (2004) Endolymph chemistry and otolith growth in fish. C R Palevol 3:535–547

Press WH, Teukolsky SA, Vetterling WT, Flannery BP (1994) Numerical recipes in Fortran. Cambridge University Press, Cambridge

Romanek C, Gauldie R (1996) A predictive model of otolith growth in fish based on the chemistry of the endolymph. Comp Biochem Physiol A 114:71–79

Ruttenberg BI, Hamilton SL, Hickford MJH, Paradis GL and others (2005) Elevated levels of trace elements in cores of otoliths and their potential for use as natural tags. Mar Ecol Prog Ser 297:273–281

Secor DH, Ohta T, Nakayama K, Tanaka M (1998) Use of otolith microanalysis to determine estuarine migrations of Japanese sea bass, *Lateolabrax japonicus*, distributed in Ariake Sea. Fish Sci 64:740–743

Skov C, Grønkjær P, Nielsen C (2001) Marking pike fry otoliths with alizarin complexone and strontium: an evaluation of methods. J Fish Biol 59:745–750

Standish JD, Sheehy M, Warner RR (2008) Use of otolith natal elemental signatures as natural tags to evaluate connectivity among open-coast fish populations. Mar Ecol Prog Ser 356:259–268

Tanner S, Reis-Santos P, Vasconcelos R, França S, Thorrold S, Cabral H (2012) Otolith geochemistry discriminates among estuarine nursery areas of *Solea solea* and *S. senegalensis* over time. Mar Ecol Prog Ser 452:193–203

Taylor HE (2001) Inductively coupled plasma-mass spectrometry: practices and techniques. Academic Press, San Diego, CA

Thorrold SR, Jones CM, Campana SE (1997) Response of otolith microchemistry to environmental variations experienced by larval and juvenile Atlantic croaker (*Micropogonias undulatus*). Limnol Oceanogr 42:102–111

Thorrold SR, Latkoczy C, Swart PK, Jones CM (2001) Natal homing in a marine fish metapopulation. Science 291: 297–299

Vroon PZ, van der Wagt B, Koornneef JM, Davies GR (2008) Problems obtaining precise and accurate Sr isotope analysis from geological materials using laser ablation MC-ICPMS. Anal Bioanal Chem 390:465–476

Waight T, Baker J, Peate D (2002) Sr isotope ratio measurements by double-focusing MC-ICPMS: techniques, observations and pitfalls. Int J Mass Spectrom 221: 229–244

Walther BD, Thorrold SR (2008) Continental-scale variation in otolith geochemistry of juvenile American shad (*Alosa sapidissima*). Can J Fish Aquat Sci 65:2623–2635

Warlen SM, Burke JS (1990) Immigration of larvae of fall/winter spawning marine fishes into a North Carolina estuary. Estuaries 13:453–461

Wells BK, Reiman BE, Clayton JL, Horan DL, Jones CM (2003) Relationships between water, otolith, and scale chemistries of Westslope cutthroat trout from the Coeur d'Alene River, Idaho: the potential application of hard-part chemistry to describe movements in freshwater. Trans Am Fish Soc 132:409–424

Woodhead J, Swearer S, Hergt J, Maas R (2005) *In situ* Sr-isotope analysis of carbonates by LA-MC-ICP-MS: interference corrections, high spatial resolution and an example from otolith studies. J Anal At Spectrom 20:22–27

Yoshinaga J, Nakama A, Morita M, Edmonds JS (2000) Fish otolith reference material for quality assurance of chemical analyses. Mar Chem 69:91–97

Zimmerman CE (2005) Relationship of otolith strontium-to-calcium ratios and salinity: experimental validation for juvenile salmonids. Can J Fish Aquat Sci 62:88–97

Zlokovitz ER, Secor DH, Piccoli PM (2003) Patterns of migration in Hudson River striped bass as determined by otolith microchemistry. Fish Res 63:245–259

Editorial responsibility: Stylianos Somarakis, Heraklion, Crete, Greece

Submitted: October 25, 2012; Accepted: March 4, 2013
Proofs received from author(s): July 2, 2013